# Interacting associations between ploidy, breeding system, and lineage diversification

Rosana Zenil-Ferguson[1,†], J. Gordon Burleigh[2], William A. Freyman[3], Boris Igić[4], Itay Mayrose[5], and Emma E. Goldberg[6]

[1]Department of Ecology, Evolution, and Behavior, University of Minnesota, Saint Paul, MN 55108, U.S.A.

[2]Department of Biology, University of Florida, Gainesville, FL 32611, U.S.A.

[3]23andMe, Inc., 899 W Evelyn Ave, Mountain View, CA 94041, U.S.A.

[4]Department of Biological Sciences, University of Illinois at Chicago, Chicago, IL 60607, U.S.A.

[5]Department of Molecular Biology and Ecology of Plants, Tel Aviv University, Tel Aviv, Israel

[6]Department of Ecology, Evolution, and Behavior, University of Minnesota, Saint Paul, MN 55108, U.S.A.

†Author for correspondence.

*Running head:* Ploidy and breeding systems in Solanaceae

*Keywords:* Polyploidy, Breeding System, Diversification, SSE models

## Abstract

If particular traits consistently affect rates of speciation and extinction, broad macroevolutionary patterns can be understood as consequences of selection at high levels of the biological hierarchy. Identifying traits associated with diversification rate differences is tricky, though, because of the many traits available to consider and the statistical challenge of testing for associations from phylogenetic data. Two traits that have been repeatedly suggested as drivers of differential diversification are whether a lineage is diploid or polyploid, and whether it is self-incompatible or self-compatible. We investigate the role of each of these traits, and their interaction, on speciation and extinction rates in Solanaceae. We find that the effect of ploidy can largely be explained by its correlation with breeding system, and that additional unknown factors work with breeding system to determine diversification rates. These results are largely robust to assumptions about whether diploidization occurs. Finally, we show that allowing for state-dependent diversification affects conclusions about the relative contribution of different evolutionary pathways to self-compatible polyploids.

## Introduction

Species accumulate around the tree of life at different rates. The search for traits that explain these differences has been accelerated by dramatic increases in phylogenetic data and, despite some setbacks (Maddison and FitzJohn 2015; Rabosky and Goldberg 2015; Moore et al. 2016), advances in analytical methods (Maddison et al. 2007; FitzJohn et al. 2009; Goldberg and Igić 2012; Beaulieu and O'Meara 2016; Rabosky and Goldberg 2017) are finding lineages where potential interesting biological processes are changing the diversification patterns.

In these studies, it is common to identify a single focal trait and investigate its association with rates of speciation and extinction. This is problematic because the context in which traits occur can lead to complex interactions amongst them. Scientists are well aware of the contribution of complex interactions to the diversification process, thus, proposing models where multivariate traits linked to diversification is necessary (see Caetano et al. (2018); Herrera-Alsina et al. (2018)).

In the present work, we focus on two of the best studied traits in flowering plants, polyploidy and breeding system and their contributions to speciation and extinction with the goal of investigating how the interaction between these two traits can illuminate the process of diversification.

Polyploidy events multiply the genomic content of cells, and have the potential to affect many other phenotypes as well as a variety of evolutionary (Ramsey and Schemske 2002) and ecological processes(Sessa 2019). Polyploidy is also a mutation that occurs commonly in plants, and it is widespread at both population and lineage scales(Husband et al. 2013; Zenil-Ferguson et al. 2017). The prevalence of chromosome number variation and ploidy change has been broadly considered as a salient feature of flowering plants for nearly a century (Stebbins 1938). The combination of ploidy changes with changes on genotypes and phenotypes raise the hypothesis that polyploidy has played an important role in shaping rates of speciation and extinction. However, when modeling polyploidy linked to diversification, statistical inferences have concluded that polyploids have slower (or even negative) rates of net diversification (speciation minus extinction) than diploids Mayrose et al. (2011, 2015). This key result was overwhelmingly consistent across 49 clades from the angiosperm phylogeny and lead to a the renaissance of the "polyploidy as an evolutionary dead-end" idea and initiated a necessary discussion about the phylogenetic location and the role of whole genome duplications in flowering plants. Genomic evidence has shown that at the base of highly diverse angiosperm clades (including the root of all angiosperms (Jiao et al. 2011)) it is possible to find at least one polyploidy event Soltis et al. (2014). Most recently, using the genomic evidence from the 1KP project (Landis et al. 2018) found 106 whole genome duplications in the angiosperm phylogeny

that combined with a state dependent diversification model resulted in approximately 60% of whole genome duplication events potentially enhancing net diversification(Landis et al. 2018). Uncovering ancient rounds of whole-genome duplications likeLandis et al. (2018) brings into question the role of genome downsizing and diploidization in the diversification process(Soltis et al. 2015; Dodsworth et al. 2015). The presence of a significant and positive net diversification rate for (some) diploids can be the result of a polyploid lineage that has been diploidized. Under this scenario, polyploidy could not longer be considered a macroevolutionary dead-end but instead, polyploidy would be the initiator of the diversification process. In the present work, we explore this polyploidy-diploidization scenario by adding diploidization rates in our proposed diversification models.

Another approach necessary to do a comprehensive evaluation of the role of polyploidy in diversification processes is the work proposed by Beaulieu and O'Meara (2016). The authors proposed models to allow for a 'hidden' or unspecified state linked to the trait of interest for models of trait linked to diversification. The presence of a hidden state can point out at sudden changes in the diversification rate under a value of a trait that are due to some unobserved source of heterogeneity and not the focal trait per se.

These hidden-state models have effectively shown that traits that were believed to be drivers of diversification, in reality are not, and that it is an unobserved but associated trait responsible for differences that are initially found. When the hidden state and not the focal trait, is responsible for changes in the diversification process, it leaves behind the question of whether the hidden state corresponds to a real state of a trait that should be sought, or whether it is an approximation of some unknowable heterogeneity, as well as whether interactions between the known and hidden trait were modeled appropriately.

Alternatively, one can simultaneously consider the effects of more than one known trait, especially in systems where multiple traits are suspected to influence diversification, and where interactions between those traits are well understood.

In the particular case of polyploidy, one of the most prominent complex interactions known is the association between ploidy and propensity for self-fertilization (Stebbins 1950). In some cases, the evidence for a correlated shift in mating system along with polyploidization appears limited and sometimes contradictory (Barringer 2007; Barrett 2008; Husband et al. 2008). In other cases, however, polyploidy is not only a suspected correlate of breeding systems but indeed a causal link (Stout and Chandler 1942; Lewis 1947). Doubled number of alleles in pollen is thought to effect disruption of the genetic mechanisms in gametophytic self-incompatibility systems, which prevent self-fertilization (Entani et al. 1999; Tsukamoto et al. 2005; Kubo et al. 2010). This creates a correlation between polyploidy and self-compatibility by precluding the existence of self-incompatible polyploids. In clades with these systems, it is thus natural to

consider the simultaneous macroevolution of polyploidy and breeding system.

Breeding system shifts—changes in the collection of physiological and morphological traits that determine the likelihood that any two gametes unite—are remarkably common and affect the distribution and amount of genetic variation in populations (Stebbins 1974; Barrett 2013). In particular, self-incompatibility systems cause a plant to reject its own pollen, and their loss, yielding self-compatibility, is one of the most replicated transitions in flowering plant evolution. Previous phylogenetic analyses have reported higher rates of diversification for self-incompatible than for self-compatible lineages (Goldberg et al. 2010; de Vos et al. 2014), but they have not considered the possibility of other correlated traits driving this pattern. Given that changes in ploidy and breeding systems may be causally related and have profound affects on the fate of lineages, it seems particularly profitable to examine possible interactions in their macroevolutionary effects. This includes their joint influence on lineage diversification, and also potential patterns in the order of their transitions. For example, do losses of SI more commonly occur tied to polyploidization, or without a ploidy shift? Do polyploids arise more commonly from self-incompatible or self-compatible diploids? Robertson et al. (2011) found that the pathway from self-incompatible diploids to self-compatible polyploids is dominated by loss of self-incompatibility followed later by polyploidization over long timescales, but proceeds in one step via polyploidization of SI species over short timescales. We revisit this question with a greatly improved phylogeny and methods that allow for diversification rate differences.

We present the most comprehensive data on ploidy and breeding system at species level in a phylogenetic context used in any trait linked diversification model. Our dataset consists of a 595 dated Solanaceae phylogeny, with ploidy and/or breeding system information for the tips of the phylogeny to investigate the associations of these two traits with lineage diversification.

In the present work, we propose a series of models that represent a comprehensive pathway of analyses that researchers need to follow when investigating complex interactions of traits in a diversification context. First, we present models where polyploidy and breeding system are modeled separatedly, and compare the resulting inferences to results of previous published models. Second, we add a hidden state to each of the models, in order to investigate if the focal trait maintains differences in diversification for focal states or if there is an unobserved but correlated hidden state that can drive the diversification pattern. Third, we ask if the hidden state is actually related to the complex interaction between breeding system and polyploidy and propose a model to consider both traits linked to diversification. In step four, we ask if on top of the complex interaction there is a second unknown trait that can be driving differences in diversication, so we add to our bivariate diversification model a hidden trait.

Finallly, we ask if diploidization can be playing a role changing patterns of diversication. We perform model selection in a Bayesian framework to identify which models are fitting better the evidence of the Solanaceae data.

## Methods

### *Data*

Chromosome number data were obtained for all Solanaceae taxa in the Chromosome Counts Database (CCDB; Rice et al. 2015), and the ca. 14,000 records were curated semi-automatically using the CCDBcurator R package (Rivero et al. 2019). CCDB contains records from original sources that have multiple complex symbol patterns denoting multivalence, or irregularites of chromosome counts. After a first full round of curation via CCDBcurator, we contrasted results by hand and corrected chromosomes where CCDBcurator's output was not able to curate. Our hand curated records were also contrasted against the large dataset Solanaceae ploidy states from Robertson et al. (2011) and against ploidy data from the C-value DNA dataset from Kew royal botanic gardens (Bennett and Leitch 2005). By contrasting three sources of information, we were able to code taxa as diploid (D) or polyploid (P). For the majority of species, ploidy was assigned according to information from the original publications and the Kew royal botanic gardens C-value DNA resource (Bennett and Leitch 2005). For taxa without ploidy information but with information about chromosome number, we assigned ploidy based on the multiplicity of chromosomes within the genus or based on information of incompatibility. If a species was incompatible without any chromosomal information it was assigned as diploid. For example, *Solanum betaceum* did not include information about ploidy level but it has 24 chromosomes, since $x = 12$ is the base chromosome number of the *Solanum* genus (Olmstead and Bohs 2007), we assigned *S. betaceum* as diploid. Species with more than one ploidy level were assigned the smallest of most frequent ploidy level recorded. Breeding system was scored as self-incompatible (I) or self-compatible (C) based on results curated from the literature and original experimental crosses (as compiled in Igić et al. 2006; Goldberg et al. 2010; Robertson et al. 2011; Goldberg and Igić 2012). Most species could unambiguously be coded as either I or C (Raduski et al. 2012). But for diploids without breeding system information taxa was coded as both I or C.Following previous work, we coded as I any species with functional I systems, even if C or dioecy was also reported. Dioecious species without functional I were coded as C.

To those existing data sets, we added some additional records for chromosome number and breeding system. The Supplementary Information contains citations for the numerous sources for the added data. Resolution of taxonomic synonymy followed the conventions provided in Solanaceae Source (PBI *Solanum*

Project 2012). Hybrids and cultivars were excluded because ploidy and breeding system can be affected by artificial selection during domestication. Following the reasoning outlined in Robertson et al. (2011), we examined closely the few species for which the merged ploidy and breeding system data indicated the presence of self-incompatible polyploids. Although I populations frequently contain some C individuals, and diploid populations frequently contain some polyploid individuals, in no case did we find a convincing case of a naturally occurring I and polyploid population. The single instance of an I and polyploid individual appears to be an allopentaploid hybrid of *Solanum oplocense* Hawkes x *Solanum gourlayii* Hawkes, reported by Camadro and Peloquin 1981. Under exceedingly rare circumstances, it is possible for polyploids containing multiple copies of S-loci to remain I, so long as they express a single allele at the S-locus (discussed in Robertson et al. 2011). Because of the resulting absence of I and polyploid populations, as well as the linked functional explanation for disabling of gametophytic self-incompatibility systems with non-self recognition, following whole genome duplication (reviewed in Ramsey and Schemske 1998; Stone 2002), we consider only three observed character states: self-incompatible diploids (ID), self-compatible diploids (CD), and polyploids which are always self-compatible (CP).

Matching our character state data to the largest time-calibrated phylogeny of Solanaceae (Särkinen et al. 2013) yielded 595 species with ploidy and/or breeding system information on the tree. Binary or three-state classification of ploidy and breeding system for the 595 taxa is summarized in Fig. 1. We retained all of these species in each of the analyses below because pruning away tips lacking breeding system in the ploidy-only analyses (and vice versa) would discard data that could inform the diversification models. A total of 405 taxa without any information about breeding system or polyploidy were excluded. Tips without trait data are much less informative for diversification parameters linked to trait values. Including this many more species would have prohibitively slowed our analyses, especially those implementing the most complex models.

### *Models for ploidy and diversification*

To investigate the association between ploidy level and diversification, we first defined a binary state speciation and extinction model (BiSSE, Maddison et al. 2007) in which taxa were classified as diploid (D) or polyploid (P) (Fig. 1). We call this the *D/P ploidy* model. In a Bayesian framework, we obtained posterior probability distributions of speciation rates ($\lambda_D$, $\lambda_P$), extinction rates ($\mu_D$, $\mu_P$), net diversification rates ($r_D = \lambda_D - \mu_D$, $r_P = \lambda_P - \mu_P$), and relative extinction rates ($v_D = \mu_D/\lambda_D$, $v_D = \mu_D/\lambda_D$) associated with each state. This analysis explores the same question as Mayrose et al. (2011, 2015), using the polyploidization (parameter $\rho$, the transition rate from D to P).

Our second model assesses the signal of diversification due to ploidy differences while also parsing

7

out the heterogeneity of diversification rates due a possible unobserved trait. BiSSE-like models can suffer from a large false discovery rate because they fail to account for diversification rate changes that do not directly depend on the trait of interest (Rabosky and Goldberg 2015; Beaulieu and O'Meara 2016). Diversification rate differences explained by some trait other than ploidy, are accommodated by adding a hidden state (HiSSE model; Beaulieu and O'Meara 2016). In this model, each of the observed diploid and polyploid states is subdivided by a binary hidden trait with states *A* and *B*. We call this the *D/P+A/B ploidy and hidden state* model. We estimated the posterior probability distributions of speciation rates ($\lambda_{D_A}$, $\lambda_{D_B}$, $\lambda_{P_A}$, $\lambda_{P_B}$), extinction rates ($\mu_{D_A}$, $\mu_{D_B}$, $\mu_{P_A}$, $\mu_{P_B}$), net diversification rates ($r_{D_A}$, $r_{D_B}$, $r_{P_A}$, $r_{P_B}$), and relative extinction rates ($\nu_{D_A}$, $\nu_{D_B}$, $\nu_{P_A}$, $\nu_{P_B}$). In this model polyploidization rate is again represented by $\rho$ and hidden states are symmetrical with rate $\alpha$.

*Models for breeding system and diversification*

To assess the effects of breeding system in the diversification process, we first fit model in which the states are self-incompatible (I) or self-compatible (C). This is the same as the analysis of Goldberg et al. (2010), save for an updated phylogeny (Särkinen et al. 2013). We call this BiSSE model the *I/C breeding system* model. To parse out the effect of breeding system on diversification, while allowing for the possibility of heterogeneous diversification rates unrelated to breeding system, we subdivided each of those states into hidden states *A* and *B*. We call this HiSSE model the *I/C+A/B breeding system and hidden state model*.

For all breeding system models, we allow transitions from *I* to *C* (at rate $q_{IC}$) but not the reverse. Within Solanaceae, self-incompatibility is homologous in all species in which S-alleles were cloned, and controlled crosses performed. All species sampled to date, possess a non-self recognition, RNase-based, gametophytic self-incompatibility (shared even with other euasterid families; Ramanauskas and Igić 2017). Furthermore, species that are distantly related within this family carry closely-related alleles, with deep trans-specific polymorphism, at the S-locus, which controls the SI response (Ioerger et al. 1990; Igić et al. 2006). This represents very strong evidence that the self-incompatible mechanism, and our *I* state is ancestral to the Solanaceae, and did not arise independently within the family ($q_{CI} = 0$).

*Models for ploidy, breeding system, and diversification*

If polyploidy and breeding system each influence lineage diversification individually, it is logical to examine their possible joint effects. We thus fit a multi-state model that includes both traits (MuSSE, FitzJohn 2012). The three states in this model are self-incompatible diploids (ID), self-compatible diploids (CD), and polyploids, which are always self-compatible (CP). As explained above, we did not include a state for self-incompatible polyploids because they are not observed in the data, and that trait combination state is

mechanistically predicted not to occur. We call this the *ID/CD/CP ploidy and breeding system* model. The model has 9 parameters, six for diversification in each state ($\lambda_{ID}$, $\lambda_{CD}$, $\lambda_{CP}$ for speciation, $\mu_{ID}$, $\mu_{CD}$, $\mu_{CP}$ for extinction) and three for transitions between states ($\rho_I$, $\rho_C$ for polyploidization transitions from *ID* and *CD* to *CP*, respectively; $q_{IC}$ for loss of self-incompatibility without polyploidization, from *ID* to *CD*). The total rate of loss of self-incompatibility, i.e., transitions out of *ID*, is $q_{IC} + \rho_I$. Diploidization from *CP* to *ID* is not allowed because it would represent a simultaneous regain of SI.

The ID/CD/CP model could potentially capture similar dynamics as earlier models, if the effects of the hidden state in D/P+A/B were effectively caused by breeding system (or its correlates), and the hidden state in I/C+A/B was effectively caused by ploidy. There is also the potential, however, for a hidden factor to be influencing diversification beyond both of our focal traits, and this could again mislead inferences. We therefore added a hidden trait layer on top of our three-state model (analogous to Caetano et al. 2018; Herrera-Alsina et al. 2018; Huang et al. 2018). We refer to this as the *ID/CD/CP+A/B* model. A fully parameterized version of this model would have 26 rate parameters (Herrera-Alsina et al. 2018). Because our goal was to look for diversification rate differences associated with ploidy and breeding system rather than the specific effects of the hidden states, we fitted a simplified version with 15 parameters. The reduction in parameter space is achieved by fixing the rates for transitions among hidden states to be equal with rate $\alpha$, and fixing the transition rates between observed states to be independent of the hidden state (rates $\rho_I$, $\rho_C$, $\delta$, $q_{IC}$ as defined for the ID/CD/CP model). There are additionally twelve diversification rate parameters ($\lambda_{ID_A}$, $\lambda_{ID_B}$, $\lambda_{CD_A}$, $\lambda_{CD_B}$, $\lambda_{CP_A}$, $\lambda_{CP_B}$, $\mu_{ID_A}$, $\mu_{ID_B}$, $\mu_{CD_A}$, $\mu_{CD_B}$, $\mu_{CP_A}$, $\mu_{CP_B}$).

### *Pathways to polyploidy*

Considering ploidy and breeding system together, there are two evolutionary pathways from SI diploid to SC polyploid (Brunet and Liston 2001; Robertson et al. 2011). In the one-step pathway, the CP state is produced directly from the ID state when whole genome duplication disables SI. In the two-step pathway, the CD state is an intermediate: SI is first lost, and later the SC diploid undergoes polyploidization. We quantify the relative contribution of these pathways to polyploidy in two ways, each using the MAP rate estimates from the IC/CD/CP model.

Both of our methods are based on a propogation matrix that describes flow from ID to CP, as in Robertson et al. (2011). We insert an artificial division in the CP state, so that one substate contains the CP species that arrived via the one-step pathway and the other substate contains the CP species that arrived via the two-step pathway. We consider only unidirectional change along each step of the pathway in order to separate them into clear alternatives, and because in this family there is no support for regain of SI, and not

9

strong support for diploidization. First, we consider only the rates of transitions between these states, placing them in the propogation matrix Q. The matrix $P = \exp(Qt)$ then provides the probabilities of changing from one state to any other state after time $t$. Closed-form solutions for the two pathway probabilities are provided in Robertson et al. (2011). Our results will differ from those of Robertson et al. (2011) because our transition rate estimates come from a dated phylogeny and a model that allows for state-dependent diversification. Second, we consider not only transitions between states but also diversification within each state. State-dependent diversification can change the relative contributions of the two pathways. In particular, if the net diversification rate is small for CD, the two-step pathway will contribute relatively less. We therefore include the difference between speciation and extinction along the diagonal elements of the propogation matrix. As before matrix exponentiation provides the relative chance of changing from one state to any other state after time $t$. In this case, however, these are not probabilities because diversification changes the number of lineages as time passes. We can still use their ratios to consider the relative contribution of each pathway, though, analogous to the normalized age structure in a growing population.

### *Diploidization as an exploratory hypothesis*

For all four models that consider ploidy changes, we allowed diploidization by adding a parameter $\delta$ connecting polyploidy state back to diploid or to self-compatible diploid in the mult-state models (denoted by $+/delta$ in the models of Table 1). Previous modeling approaches (Mayrose et al. 2011) have argued against inferring diploidization rates when using ploidy data that comes from classifications based on chromosome number multiplicity or chromosome number change models like chromEvol (Mayrose et al. 2010). These types of classifications do not allow for a ploidy reversion. Where indicated, the classification of ploidy for the data used in our models was based on chromosome multiplicity at the genus level. However, the majority of the ploidy classifications were adopted from original studies with alternative sources of information (e.g., geographic distribution, genus ploidy distribution) where ploidy was defined by authors that found evidence for it. Since it is not clear whether diploidization can be detected under alternative ploidy classifications or even classifications based on chromosome number multiplicity at the genus level, we also fit the models without diploidization in order to test whether the conclusions about diversification are sensitive to including diploidization. As discussed by Servedio et al. (2014), the presence or absence of a hypothesis can have an exploratory goal. In our case the diploidization parameter (or its absence, $\delta = 0$) in our models is an opportunity to explore an assumption that might be important but that is not the single definitive process to understand the interactions among polyploidy, breeding system, and diversification.

10

*Statistical inference under the models*

Parameters for each of the 10 diversification models were estimated using custom code in the RevBayes (Höhna et al. 2016) environment. Code for analyses and key results is available at `https://github.com/roszenil/solploidy`. We included a correction for incomplete sampling in all analyses, based on assuming that the Solanaceae family has approximately 3,000 species ($s = 595/3000$) as estimated by the Solanaceae Source project (PBI *Solanum* Project 2012). For all 10 models, we assumed that speciation and extinction parameters had log-normal prior distributions with means equal to the expected net diversification rate (number of taxa/[$2 \times$ root age]) and standard deviation 0.5. Priors for parameters defining trait changes were assumed to be gamma distributed with parameters $k = 0.5$ and $\theta = 1$. For each model, an MCMC chain was run for 96 hours in the high-performance computational cluster at the Minnesota Supercomputing Institute, which allowed for 5,000 generations of burn-in and a minimum of 200,000 generations of MCMC for each of the 10 models. For each model, convergence and mixing of the MCMC was tested using the R library `coda` and the software package Tracer (see supplementary information for convergence plots).

In the RevBayes code we calculated the probability of ancestral states at each node as performed chromosome number change models proposed in Freyman and Hoehna (2017). Ancestral reconstructions for all models can be found in the supplementary information and show the maximum a posteriori of the marginal probability distributions for each of the 594 internal nodes for each of the 10 models.

*Model selection*

We calculated the marginal likelihood for each of the 10 models in RevBayes (Höhna et al. 2016). Marginal likelihoods were calculated using 50 stepping stone steps under the methodology of Xie et al. (2010). Each stepping stone step was found by calculating 500 generations of burn-in followed by a total of 1,000 MCMC steps (Table 1). The calculation of each marginal likelihood ran for 24 hours on a high-performance computational cluster.

Using the marginal likelihood values, we calculated thirteen different Bayes factors. Six compared the models of ploidy against one other (D/P and D/P+A/B, each with or without diploidization), one compared the breeding system models (I/C and I/C+A/B), and six compared the models with both traits (ID/CD/CP and ID/CD/CP+A/B, each with or without diploidization) (Table 2). Other comparisons between these models are not valid because the input data are different under the different state space codings (Fig. 1). In mathematical terms, the D/P, I/C, and ID/CD/CP state spaces are not 'lumpable' with respect to one another (Tarasov 2018). Each model comparison is reported with a Bayes factor on the natural log scale: the comparison between models $M_0$ and $M_1$ is $BF(M_0, M_1) = \ln[P(\mathbf{X}|M_0) - P(\mathbf{X}|M_1)]$. There is 'positive'

support for $M_0$ when this value is more than 2, 'strong' support when it is more than 6, and 'very strong' support when it is more than 10 (Kass and Raftery 1995).

## Results

### *Traits and diversification*

Individual trait-dependent diversification inference, of ploidy and breeding system considered separately, each showed significant associations with net diversification differences. When considered together, how-ever, the effect of breeding system dominated the effect of ploidy, although hidden factors played an impor-tant role as well.

When considering ploidy alone (D/P model), we found a greater net diversification rate for diploids than for polyploids, in agreement with (Mayrose et al. 2011, 2015). This result holds with (Fig. 2A) or without (Fig. 3A) the diploidization parameter, though including diploidization shifts the net diversification rate of polyploids to be non-negative. Incorporating a hidden state, however, removes the clear separation in diversification between diploids and polyploids (D/P+A/B model; Fig. 2B, Fig. 3B). Thus, differences in net diversification are better explained by an unknown factor than by ploidy. Statistical model comparisons show very strong support for including the hidden state and strong support for including diploidization (Table 2).

When considering breeding system alone (I/C model, Fig. 2C), we found a larger net diversification rate for SI than for SC species, in agreement with Goldberg et al. (2010). When a hidden state is included (I/C+A/B model), the large net diversification difference persists for one of the hidden states but is removed for the other (Fig. 2D). Thus, differences in net diversification are best explained by both breeding system and an unknown factor. The statistical model comparison shows very strong support for including the hidden state (Table 2).

When considering ploidy and breeding system together (ID/CD/CP model), the net diversification rate for SI diploids was greater than for either SC diploids or SC polyploids, with or without diploidization (Fig. 2E, Fig. 3C). It thus appears that the difference in net diversification with breeding system persists when ploidy is included in the model, but not the reverse. The association of ploidy with net diversification in the D/P model (Fig. 2A, Fig. 3A) appears to be driven by the subset of diploids that are SI; among SC species, net diversification rates for diploids and polyploids are similar. When a hidden state is included (IC/CD/CP+A/B model), the same general pattern remains when diploidization is prevented (Fig. 3D), although the higher net diversification rate of ID is less clear within one of the hidden states. With diploidization, the net diversification rate of ID is still greater than CD within each hidden state, but diversification for P is highly

12

uncertain and perhaps bimodal. Statistical model comparisons show very strong support for including the hidden state and at most positive support for including diploidization (Table 2).

*Pathways to polyploidy*

Evolution from self-incompatible diploids to self-compatible polyploids can proceed through two different pathways. Determining the relative contribution of these pathways based on our estimated transition rates from the ID/CD/CP model, we find that the one-step pathway is more likely on short timescales and the two-step pathway is more likely on long timescales (Fig. 4, left panels). When not much time has elapsed, the one-step pathway is more likely because only one event need happen. When more time has elapsed, the two-step pathway is more likely because the rate of loss of SI within diploids, $q_{IC}$, is greater than the rate of polyploidization for SI species, $\rho_I$ (Fig. S7). These conclusions are the same as those of Robertson et al. (2011) under one of their branch length approximations.

When rates of lineage diversification are considered, however, the conclusions change. Even over long timescales, the two-step pathway contributes less (Fig. 4, right panels). The lower rate of net diversification in the CD state, relative to ID, means that relatively fewer lineages are available to complete the second step of the two-step pathway.

*Diploidization as an exploratory hypothesis*

We considered models both with or without diploidization in order to explore the effects of this process on the estimates of state-dependent diversification. For the two models that only include diploid and polyploid states (D/P and D/P+A/B), the net diversification rate of polyploid lineages is likely negative when diploidization (parameter $\delta$) is excluded but positive when $\delta$ is included (Fig. 2A versus Fig. 3A). For the two models that also included breeding system (ID/CD/CP and ID/CD/CP+A/B), the main effect of including diploidization is increasing the uncertainty of the estimate of polyploid net diversification rate (Fig. 2EF versus Fig. 3CD). For all models, there is greater uncertainty in the estimate of diploidization rate than polyploidization rate, as judged by the width of the credibility intervals (see supplementary information figures).

## Discussion

The present work shows the importance of considering the trait linked diversification patterns under a multivariate approach. Species are created and go extinct based un multiple and often highly correlated phenotypes, understanding the speciation and extinction processes requires understanding of the evolutionary consequences that those trait correlations produce in organisms. In the present work we show how consider-

13

ing both polyploidy and breeding system can disentangle the importance (or the lack of) of polyploidy when confronted with the evidence brought by breeding system.

Using the most complete dataset for polyploidy in a phylogenetic tree in Solanaceae, we were able to replicate the results found by Mayrose et al. (2011), polyploids have a slower net diversification compare to diploids. Furthermore, we also found polyploids had a high probability of having negative diversification which implies that polyploids can become a macroevolutionary dead-end, a result that was also found in the two large angiosperm diversification studies Mayrose et al. (2011) and Mayrose et al. (2015). However, we expanded this study to accommodate background heterogeneity in the diversification process. When adding heterogeneity we found that it was more likely that an unobserved trait linked to diploid state was the one leading the net diversification patterns, and that there were some "second-class" diploids that were not different from polyploids in diversification terms (Figure 2A). This result lead us to our central question: *what is that other trait linked diploids that makes them different in the diversification process?* .

In Solanaceae, our immediate intuition was to look into breeding system. Previous studies shown that self-incompatible Solanaceae species have also higher rates of diversification compared to their self-compatible counterparts (Goldberg and Igić 2012). Self-incompatible species are diploid in our sample and also expected to be diploid due to ... (citation?). By considering both polyploidy and breeding system simultaneously for every species in our sample, it was possible to disentangle why some diploids were quantitatively different than polyploids. In the three-state diversification model ID/CD/CP, we found that self-incompatible diploids have faster and positive rates than self-compatible diploids and polyploids, and that the difference between the rates of net diversification of self-compatible diploids is not as large (Figures 2C) as first found by binary trait diversification models (Figures 2A). This result is important, since it aligns with the net diversification results of the D/P+A/B model, where a ' 'hidden-trait" seem to be dictating the diversification pattern. By adding breeding system, we were able to hint at which that hidden-trait possibly is. Therefore, we consider that finding a heterogenous result in the hidden trait approaches should be be treated as evidence of a second trait that is necessary to consider. Pursuing knowledge of such trait can result on a clearer picture of the importance of trait linked diversification patterns, but also on a better reconstruction on past events in phylogenies.

Diploidization needs to be considered in diversification models because higher rates of net diversification (speciation minus extinction) in diploids can be obtained from models that ignore the possibility of a polyploid lineage that has diploidized being the diversification enhancer. Hence, in a diploidization lacking model, diploids will show higher rates of diversification when in fact it is a polyploidy event and its subsequent diploidization that generated higher speciation and less extinction. By adding diploidization

14

to models of polyploidy linked to diversification it is possible to recover this complicated scenario and to reconcile genomic evidence with stochastic models.

Diploidization is widely considered to be relatively rare, compared with polyploidization, but flowering plant lineages are thought to have experienced at least one round of polyploidization in their evolutionary history. As a consequence, it is possible that nearly all extant species classified as "diploid" in our analyses are possibly secondary diploids, having undergone both polyploidization and re-diploidization. Genomic evidence indicates that such an event may have occurred prior to the origin of the family Solanaceae. Ku et al. (2000) and Blanc and Wolfe (2004) posited that the lineage leading to tomato, *Solanum lycopersicum*, may have experienced one or more paleopolyploid events. A subsequent analysis of synteny between grape and *Solanum* genomes, as well as the distribution between inferred paralogs within *Solanum* (tomato and potato) genomes both suggest that this lineage experienced a likely round of ancient genome duplication or triplication (Tomato Genome Consortium 2012). The age of the peak of paralog Ks distances, is approximately 71 million years (Tomato Genome Consortium 2012). If this is the case, then all of the genomes may have been subsequently re-diploidized, because common base chromosome numbers this and related families are n=11-12. On the other hand, studies comparing map-based genome synteny within the family find no evidence for recent polyploidization-diploidization (Wu and Tanksley 2010). Simple genome re-arrangements appear sufficient to explain chromosomal evolution between a number of species, including all of those in the relatively cytogenetically conserved 'x=12' group, which includes tomato, potato, eggplant, pepper, and tobacco.

## Acknowledgements

## Literature Cited

Barrett, S. C., 2008. Major evolutionary transitions in flowering plant reproduction: an overview.

———, 2013. The evolution of plant reproductive systems: how often are transitions irreversible? Proceedings of the Royal Society B: Biological Sciences 280:20130913.

Barringer, B. C., 2007. Polyploidy and self-fertilization in flowering plants. American Journal of Botany 94:1527–1533.

Beaulieu, J. M. and B. C. O'Meara, 2016. Detecting hidden diversification shifts in models of trait-dependent speciation and extinction. Syst Biol 65:583–601.

Bennett, M. D. and I. J. Leitch, 2005. Plant DNA C-values database.

Blanc, G. and K. H. Wolfe, 2004. Widespread paleopolyploidy in model plant species inferred from age distributions of duplicate genes. The Plant Cell 16:1667–1678.

Brunet, J. and A. Liston, 2001. Technical comment on polyploidy and gender dimorphism. Science 291:1441–1442.

Caetano, D. S., B. C. O'Meara, and J. M. Beaulieu, 2018. Hidden state models improve state-dependent diversification approaches, including biogeographical models. Evolution 72:2308–2324.

Camadro, E. and S. J. Peloquin, 1981. Cross-incompatibility between two sympatric polyploid *Solanum* species. Theoretical and Applied Genetics 60:65–70.

Dodsworth, S., M. W. Chase, and A. R. Leitch, 2015. Is post-polyploidization diploidization the key to the evolutionary success of angiosperms? Botanical Journal of the Linnean Society 180:1–5.

Entani, T., S. Takayama, M. Iwano, H. Shiba, F.-S. Che, and A. Isogai, 1999. Relationship between polyploidy and pollen self-incompatibility phenotype in *Petunia hybrida* Vilm. Bioscience, Biotechnology, and Agrochemistry 63:1882–1888.

FitzJohn, R. G., 2012. Diversitree : comparative phylogenetic analyses of diversification in r. Methods Ecol Evol 3:1084–1092.

FitzJohn, R. G., W. P. Maddison, and S. P. Otto, 2009. Estimating trait-dependent speciation and extinction rates from incompletely resolved phylogenies. Systematic Biology 58:595–611.

Freyman, W. and S. Hoehna, 2017. Stochastic character mapping of state-dependent diversification reveals the tempo of evolutionary decline in self-compatible lineages. BioRxiv .

Goldberg, E. E. and B. Igić, 2012. Tempo and mode in plant breeding system evolution. Evolution 66:3701–3709.

Goldberg, E. E., J. R. Kohn, R. Lande, K. A. Robertson, S. A. Smith, and B. Igić, 2010. Species selection maintains self-incompatibility. Science 330:493–495.

Herrera-Alsina, L., P. van Els, and R. S. Etienne, 2018. Detecting the dependence of diversification on multiple traits from phylogenetic trees and trait data. Systematic biology .

Höhna, S., M. J. Landis, T. A. Heath, B. Boussau, N. Lartillot, B. R. Moore, J. P. Huelsenbeck, and F. Ronquist, 2016. Revbayes: Bayesian phylogenetic inference using graphical models and an interactive model-specification language. Systematic Biology 65:726–736.

Huang, D., E. E. Goldberg, L. Chou, and K. Roy, 2018. The origin and evolution of coral species richness in a marine biodiversity hotspot. Evolution 72:288–302.

Husband, B. C., S. J. Baldwin, and J. Suda, 2013. The incidence of polyploidy in natural plant populations: major patterns and evolutionary processes. Pp. 255–276, *in* Plant Genome Diversity Volume 2. Springer.

Husband, B. C., B. Ozimec, S. L. Martin, and L. Pollock, 2008. Mating consequences of polyploid evolution in flowering plants: Current trends and insights from synthetic polyploids. International Journal of Plant Sciences 169:195–206.

Igić, B., L. Bohs, and J. R. Kohn, 2006. Ancient polymorphism reveals unidirectional breeding system shifts. Proc Natl Acad Sci USA 103:1359–1363.

Ioerger, T. R., A. G. Clark, and T. H. Kao, 1990. Polymorphism at the self-incompatibility locus in Solanaceae predates speciation. Proceedings of the National Academy of Sciences USA 87:9732–9735.

Jiao, Y., N. J. Wickett, S. Ayyampalayam, A. S. Chanderbali, L. Landherr, P. E. Ralph, L. P. Tomsho, Y. Hu, H. Liang, P. S. Soltis, et al., 2011. Ancestral polyploidy in seed plants and angiosperms. Nature 473:97.

Kass, R. E. and A. E. Raftery, 1995. Bayes factors. Journal of the American Statistical Association 90:773–795.

Ku, H. M., T. Vision, J. Liu, and S. D. Tanksley, 2000. Comparing sequenced segments of the tomato and *Arabadopsis* genomes: large-scale duplication followed by selective gene loss creates a network of synteny. Proceedings of the National Academy of Science, USA 97:9121–9126.

Kubo, K.-i., T. Entani, A. Takara, N. Wang, A. M. Fields, Z. Hua, M. Toyoda, S.-i. Kawashima, T. Ando, A. Isogai, et al., 2010. Collaborative non-self recognition system in s-rnase–based self-incompatibility. Science 330:796–799.

Landis, J. B., D. E. Soltis, Z. Li, H. E. Marx, M. S. Barker, D. C. Tank, and P. S. Soltis, 2018. Impact of whole-genome duplication events on diversification rates in angiosperms. American Journal of Botany 105:348–363.

Lewis, D., 1947. Competition and dominance of incompatibility alleles in diploid pollen. Heredity 1:85–108.

Maddison, W. P. and R. G. FitzJohn, 2015. The unsolved challenge to phylogenetic correlation tests for categorical characters. Systematic Biology 64:127–136.

Maddison, W. P., P. E. Midford, and S. P. Otto, 2007. Estimating a binary character's effect on speciation and extinction. Syst Biol 56:701–710.

Mayrose, I., M. S. Barker, and S. P. Otto, 2010. Probabilistic models of chromosome number evolution and the inference of polyploidy. Systematic Biology 59:132–144.

Mayrose, I., S. H. Zhan, C. J. Rothfels, N. Arrigo, M. S. Barker, L. H. Rieseberg, and S. P. Otto, 2015. Methods for studying polyploid diversification and the dead end hypothesis: a reply to soltis et al. (2014). New Phytol 206:27–35.

Mayrose, I., S. H. Zhan, C. J. Rothfels, K. Magnuson-Ford, M. S. Barker, L. H. Rieseberg, and S. P. Otto, 2011. Recently formed polyploid plants diversify at lower rates. Science 333:1257.

Moore, B. R., S. Höhna, M. R. May, B. Rannala, and J. P. Huelsenbeck, 2016. Critically evaluating the theory and performance of bayesian analysis of macroevolutionary mixtures. Proceedings of the National Academy of Sciences 113:9569–9574.

Olmstead, R. G. and L. Bohs, 2007. A summary of molecular systematic research in Solanaceae: 1982–2006. Acta Horticulturae Pp. 255–268.

PBI *Solanum* Project, 2012. Solanaceae Source: a global taxonomic resource for the nightshade family.

Rabosky, D. L. and E. E. Goldberg, 2015. Model inadequacy and mistaken inferences of trait-dependent speciation. Systematic Biology 64:340–355.

———, 2017. Fisse: A simple nonparametric test for the effects of a binary character on lineage diversification rates. Evolution 71:1432–1442.

Raduski, A. R., E. B. Haney, and B. Igić, 2012. The expression of self-incompatibility in angiosperms is bimodal. Evolution 66:1275–1283.

Ramanauskas, K. and B. Igić, 2017. The evolutionary history of plant t2/s-type ribonucleases. PeerJ 5:e3790.

Ramsey, J. and D. W. Schemske, 1998. Pathways, mechanisms, and rates of polyploid formation in flowering plants. Annual Review of Ecology and Systematics 29:467–501.

———, 2002. Neopolyploidy in flowering plants. Annual review of ecology and systematics 33:589–639.

Rice, A., L. Glick, S. Abadi, M. Einhorn, N. M. Kopelman, A. Salman-Minkov, J. Mayzel, O. Chay, and

I. Mayrose, 2015. The chromosome counts database (CCDB) - a community resource of plant chromosome numbers. New Phytol 206:19–26.

Rivero, R., E. B. Sessa, and R. Zenil-Ferguson, 2019. Eyechrom and ccdb curator: Visualizing chromosome count data from plants. Applications in Plant Sciences P. e01207.

Robertson, K., E. E. Goldberg, and B. Igić, 2011. Comparative evidence for the correlated evolution of polyploidy and self-compatibility in solanaceae. Evolution 65:139–155.

Särkinen, T., L. Bohs, R. G. Olmstead, and S. Knapp, 2013. A phylogenetic framework for evolutionary study of the nightshades (Solanaceae): a dated 1000-tip tree. BMC Evol Biol 13:214.

Servedio, M. R., Y. Brandvain, S. Dhole, C. L. Fitzpatrick, E. E. Goldberg, C. A. Stern, J. Van Cleve, and D. J. Yeh, 2014. Not just a theory?the utility of mathematical models in evolutionary biology. PLoS biology 12:e1002017.

Sessa, E. B., 2019. Polyploidy as a mechanism for surviving global change. New Phytologist 221:5–6.

Soltis, D. E., M. C. Segovia-Salcedo, I. Jordon-Thaden, L. Majure, N. M. Miles, E. V. Mavrodiev, W. Mei, M. B. Cortez, P. S. Soltis, and M. A. Gitzendanner, 2014. Are polyploids really evolutionary dead-ends (again)? a critical reappraisal of mayrose et al.(2011). New Phytologist 202:1105–1117.

Soltis, P. S., D. B. Marchant, Y. Van de Peer, and D. E. Soltis, 2015. Polyploidy and genome evolution in plants. Current opinion in genetics & development 35:119–125.

Stebbins, G. L., 1938. Cytological characteristics associated with the different growth habits in the dicotyledons. American Journal of Botany 25:189–198.

———, 1950. Variation and Evolution in Plants. Columbia University Press, New York.

———, 1974. Flowering plants: evolution above the species level. Belknap Press of Harvard University Press, Cambridge, Mass.

Stone, J. L., 2002. Molecular mechanisms underlying the breakdown of gametophytic self-incompatibility. The Quarterly Review of Biology 77:17–30.

Stout, A. B. and C. Chandler, 1942. Hereditary transmission of induced tetraploidy and compatibility in fertilization. Science 96:257–258.

Tarasov, S., 2018. Integration of anatomy ontologies and evo-devo using structured markov models suggests a new framework for modeling discrete phenotypic traits. BioRxiv P. 188672.

Tomato Genome Consortium, 2012. The tomato genome sequence provides insights into fleshy fruit evolution. Nature 485:635.

Tsukamoto, T., T. Ando, H. Watanabe, E. Marchesi, and T.-h. Kao, 2005. Duplication of the s-locus f-box gene is associated with breakdown of pollen function in an s-haplotype identified in a natural population of self-incompatible petunia axillaris. Plant Molecular Biology 57:141–153.

de Vos, J. M., C. E. Hughes, G. M. Schneeweiss, B. R. Moore, and E. Conti, 2014. Heterostyly accelerates diversification via reduced extinction in primroses. Proceedings of the Royal Society B: Biological Sciences 281:20140075.

Wu, F. and S. D. Tanksley, 2010. Chromosomal evolution in the plant family solanaceae. BMC Genomics 11:182.

Xie, W., P. O. Lewis, Y. Fan, L. Kuo, and M.-H. Chen, 2010. Improving marginal likelihood estimation for bayesian phylogenetic model selection. Systematic biology 60:150–160.

Zenil-Ferguson, R., J. M. Ponciano, and J. G. Burleigh, 2017. Testing the association of phenotypes with polyploidy: An example using herbaceous and woody eudicots. Evolution 71:1138–1148.
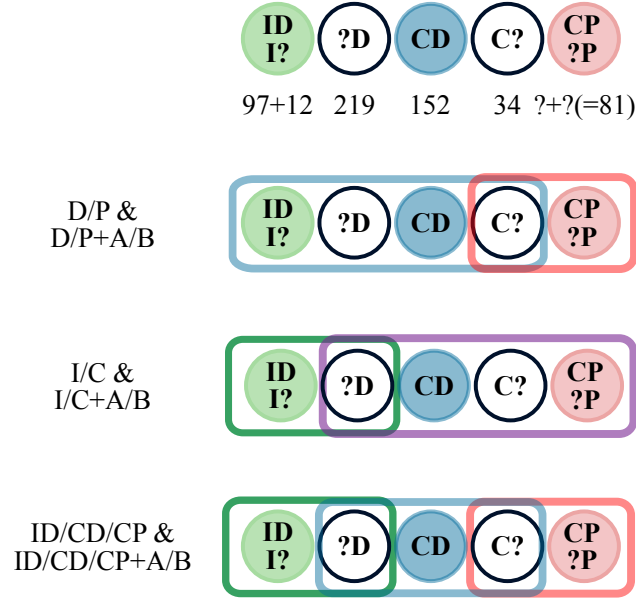
Figure 1: Character states used for each of the models. Each species retained on the tree belonged to one of five possible categories, depending on whether ploidy and/or breeding system were known. The number of species in each is shown under the corresponding circles in the top row. These categories were then grouped in a manner appropriate to the states of each model. For example, there are 34 species that are self-compatible and of unknown ploidy; these are coded as either *D* or *P* in the D/P models (uncertain, or consistent with either state), as *C* in the I/C models, and as either *CD* or *CP* in the ID/CD/CP models. In all cases, species were coded as either *A* or *B* in the hidden state models. The models depicted in the different rows use state spaces that are not comparable with one another. For example, we cannot test whether the D/P model fits better than the I/C model because they use states that are not the same and are not 'lumpable' (Tarasov 2018).
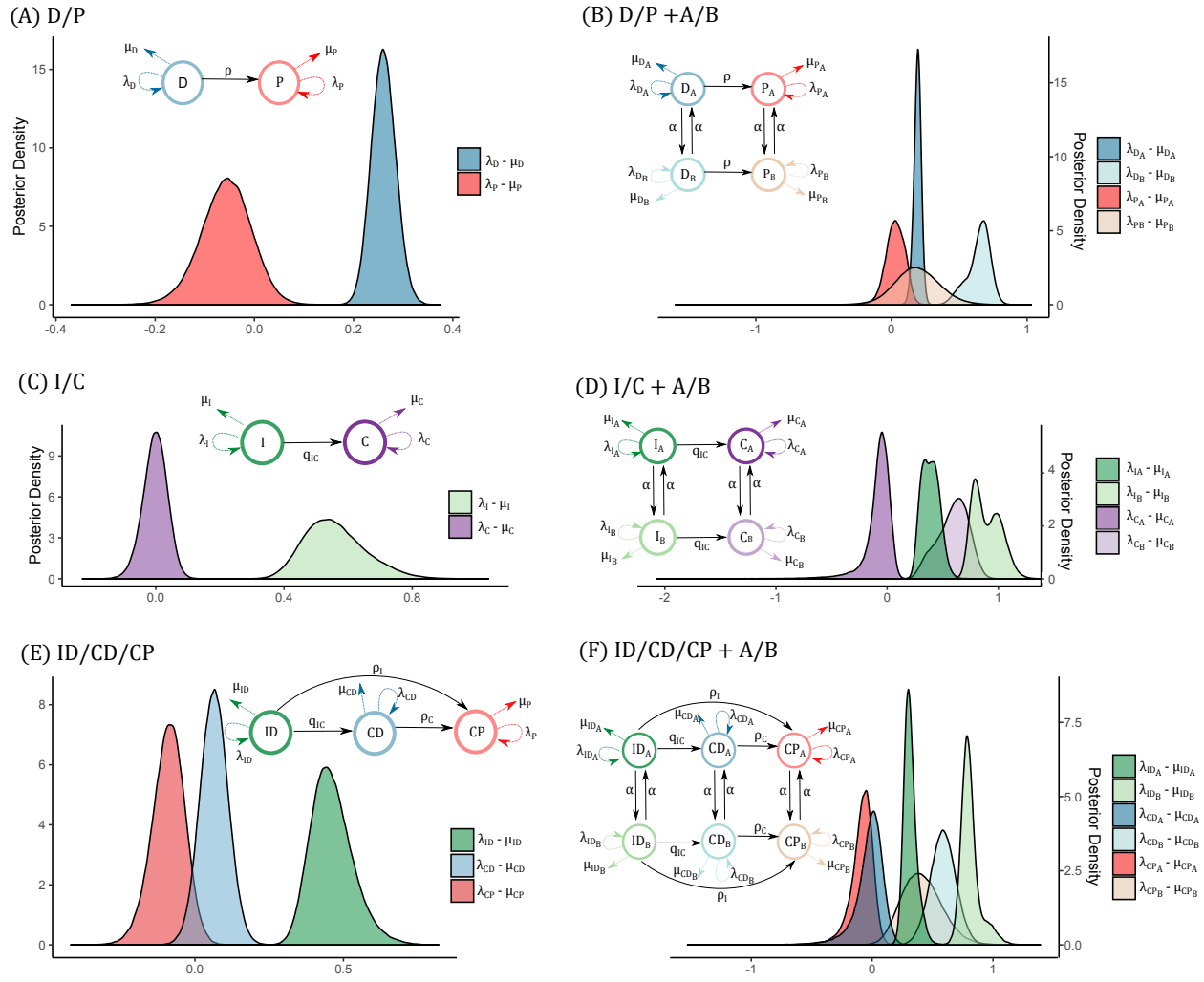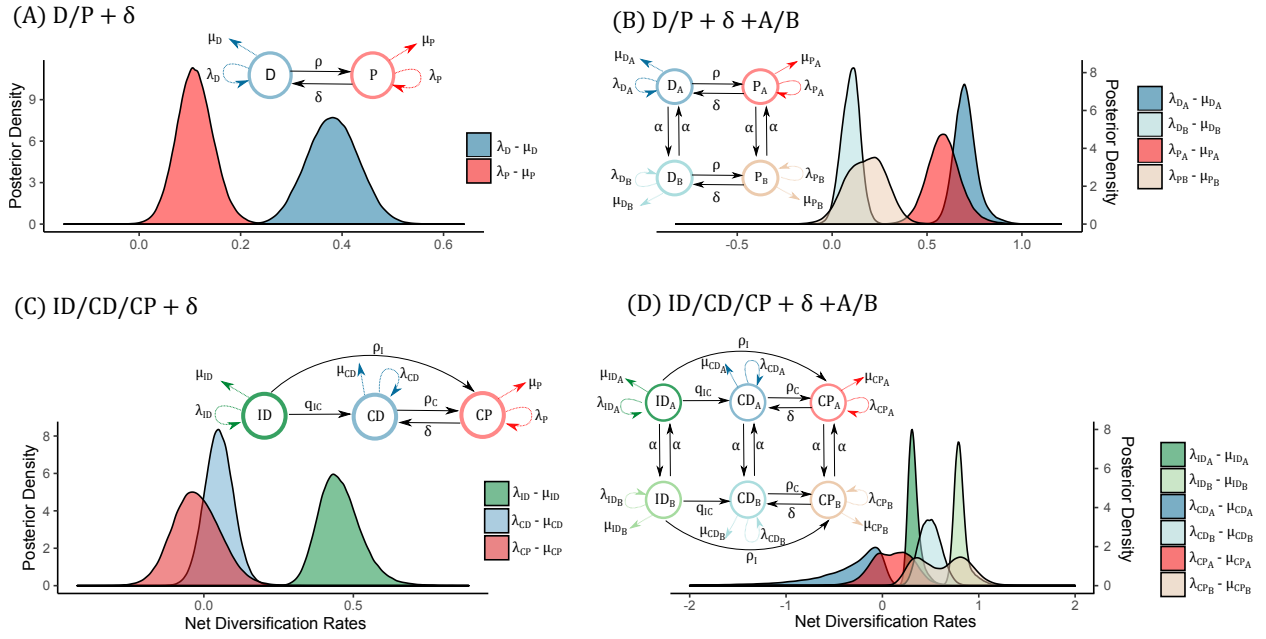
Figure 2: Net diversification rates for all models.

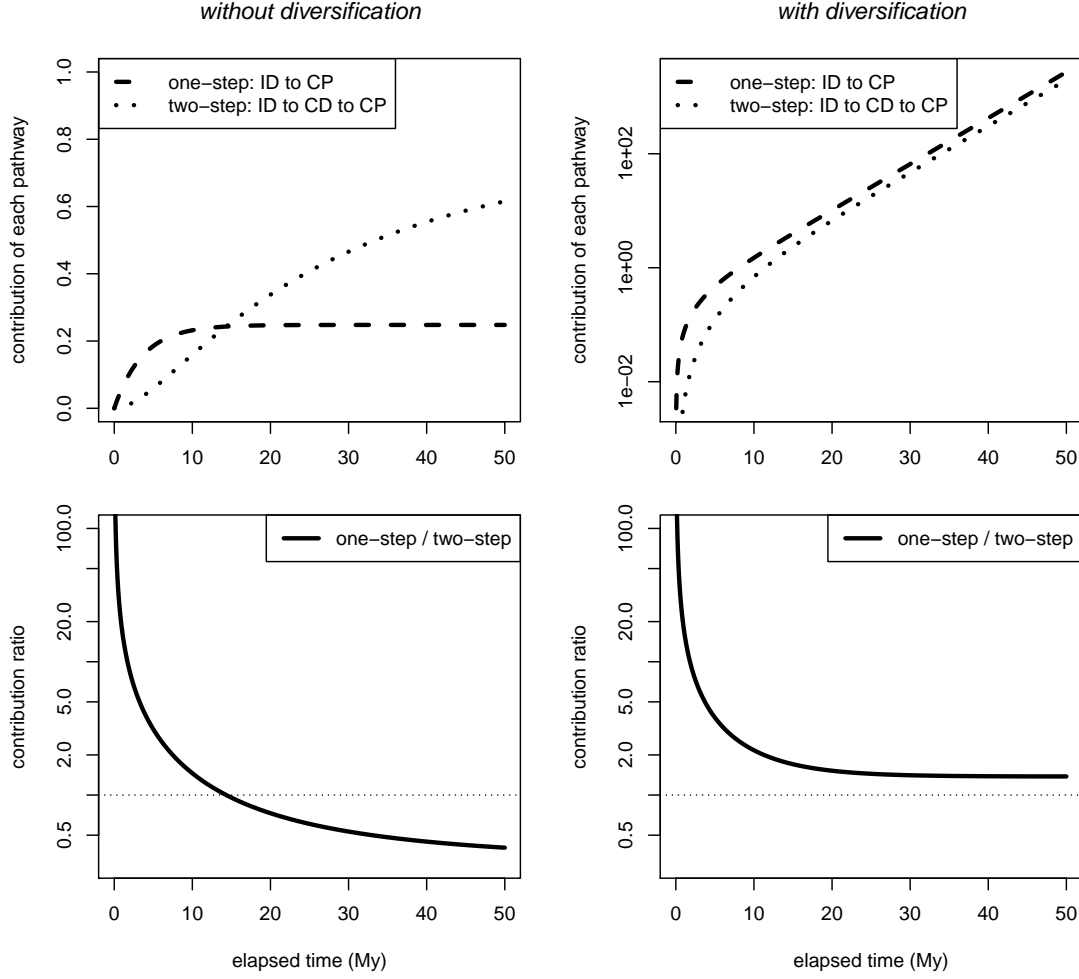Figure 3: Net diversification rates for all models that include diploidization.

Figure 4: Contributions of the two pathways to polyploidy, the one-step ID→CP transitions, and the two-step, ID→CD→CP transitions. Panel (a) shows the contributions when considering only transition rates among the states (ignoring the diversification rate parameters). The one-step pathway dominates on short timescales and the two-step on long timescales. Panels (b) shows the contributions when including diversification of lineages in each state. The one-step pathway, in which polyploidy breaks down SI, dominates over any timescale. Panels (c) and (d) plot the ratio of the pathway contributions in the upper panels, (a) and (b), respectively.

| Model | Ploidy | Diploidization | Breeding System | Hidden State | Num Parameters | Marginal Log-Likelihood |
|---|---|---|---|---|---|---|
| 1. D/P | Yes | No | No | No | 5 | -1193.66 |
| 2. D/P +$\delta$ | Yes | Yes | No | No | 6 | -1182.93 |
| 3. D/P+A/B | Yes | No | No | Yes | 10 | -1150.99 |
| 4. D/P+$\delta$+A/B | Yes | Yes | No | Yes | 11 | **-1145.69** |
| 5. I/C | No | No | Yes | No | 5 | -1194.80 |
| 6. I/C+A/B | No | No | Yes | Yes | 10 | **-1155.37** |
| 7. ID/CD/CP | Yes | No | Yes | No | 9 | -1345.87 |
| 8. ID/CD/CP +$\delta$ | Yes | Yes | Yes | No | 10 | -1344.50 |
| 9. ID/CD/CP+A/B | Yes | No | Yes | Yes | 15 | -1303.55 |
| 10. ID/CD/CP+$\delta$+A/B | Yes | Yes | Yes | Yes | 16 | **-1300.35** |

Table 1: The ten models and their marginal likelihoods. Values in bold are for the best models within each class that are comparable (see Table 2). Abbreviations are D: diploid, P: polyploid, I: self-incompatible, C: self-compatible, A: one state of hidden trait, B: other state of hidden trait, $\delta$: diploidization.

| Ploidy Models | | | | Breeding System Models | | Ploidy and Breeding System Models | | | |
|---|---|---|---|---|---|---|---|---|---|
| 1 | 2 | 3 | 4 | 5 | 6 | 7 | 8 | 9 | 10 |
| 1. D/P · | 10.72 | -37.24 | -31.94 | 5. I/C · | -39.43 | 7. ID/CD/CP · | 1.36 | -44.15 | -40.95 |
| 2. D/P no $\delta$ · | · | -47.97 | -42.66 | **6. I/C+A/B** · | · | 8. ID/CD/CP no $\delta$ · | · | -45.51 | -42.31 |
| **3. D/P+A/B** · | · | · | 5.30 | | | **9. ID/CD/CP+A/B** · | · | · | 3.2 |
| 4. D/P+A/B no $\delta$ · | · | · | · | | | 10. ID/P/CD no $\delta$-A/B · | · | · | · |

Table 2: Bayes factors for model comparisons. Each of the three boxes contains models that can be compared with one another, based on the character states they include (see Fig. 1). Models are numbered in as Table 1. Bayes factors are reported on the natural log scale, so numbers greater than $+2$ mean that the model in the row label has 'positive' support relative to the model in the column label; numbers less than $-2$ mean that model in the column label is the preferred one. Conventional thresholds for 'strong' and 'very strong' support are 6 and 10, respectively. The best model in each set is written in bold. In each case, it is the most complex model of the set.
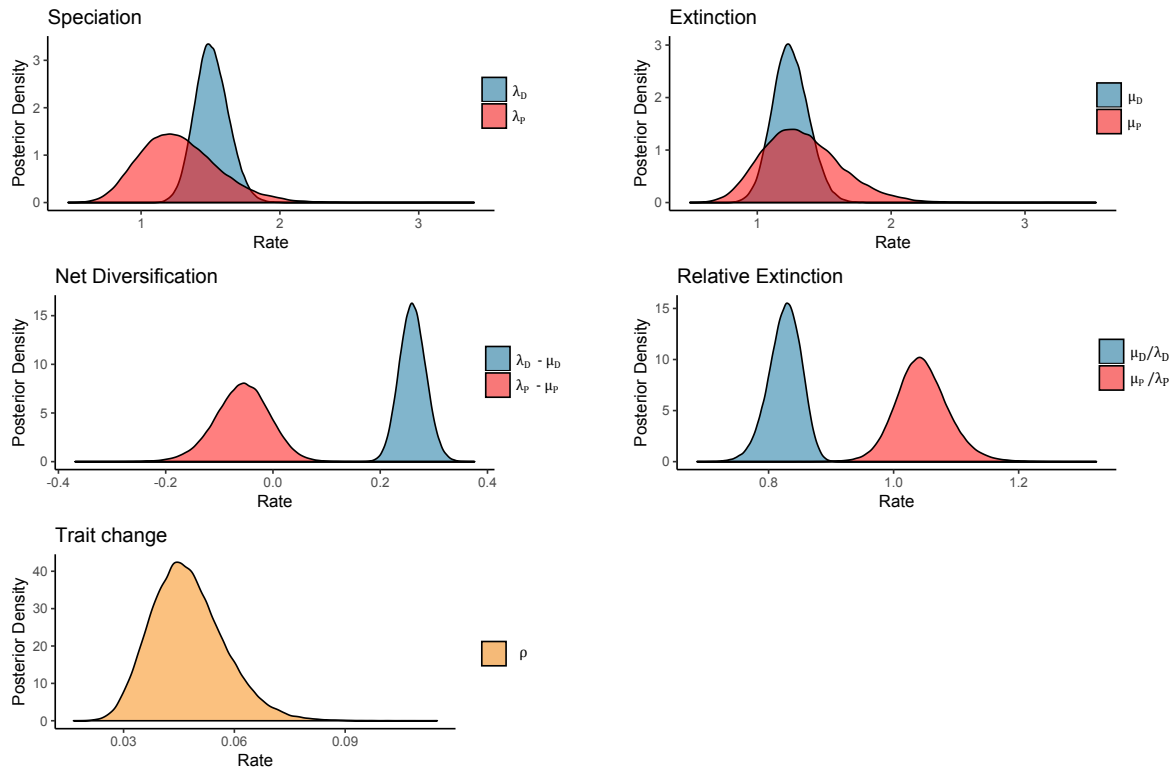
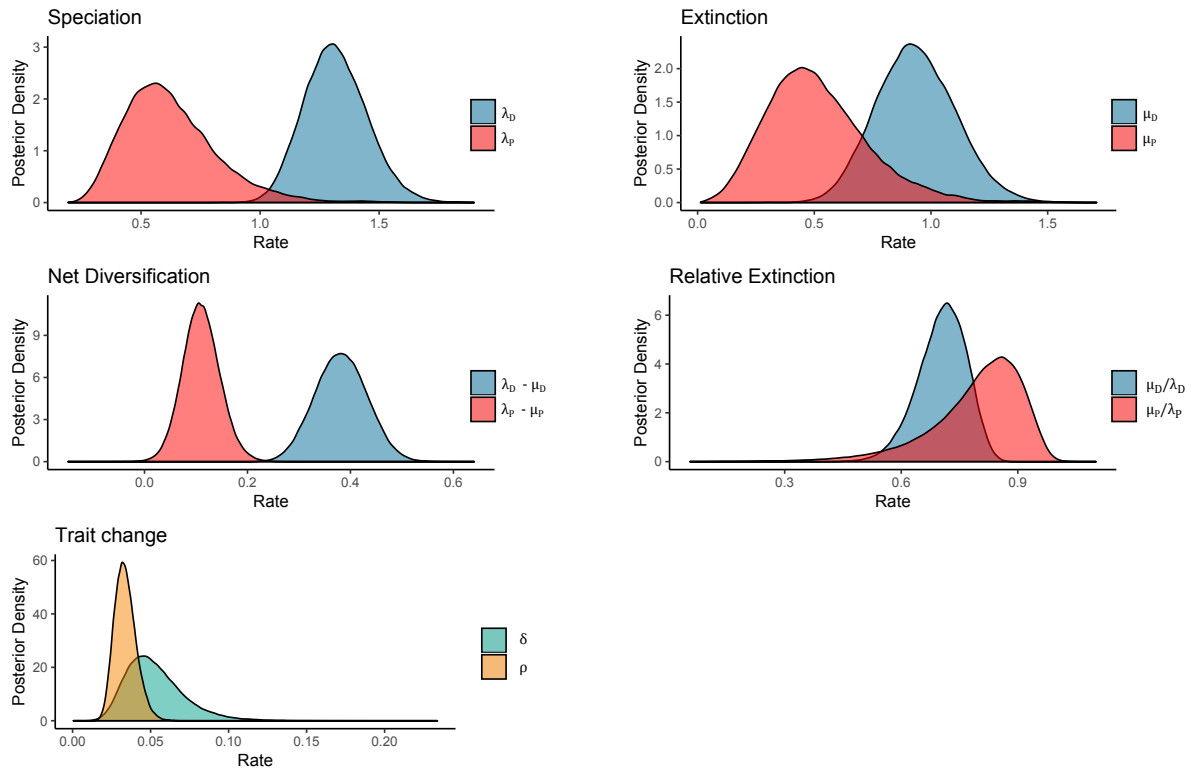Figure S1: Posterior distribution for each of the parameters in the D/P, polyploidy model

Figure S2: Posterior distribution for each of the parameters in the D/P+ $\delta$,polyploidy model
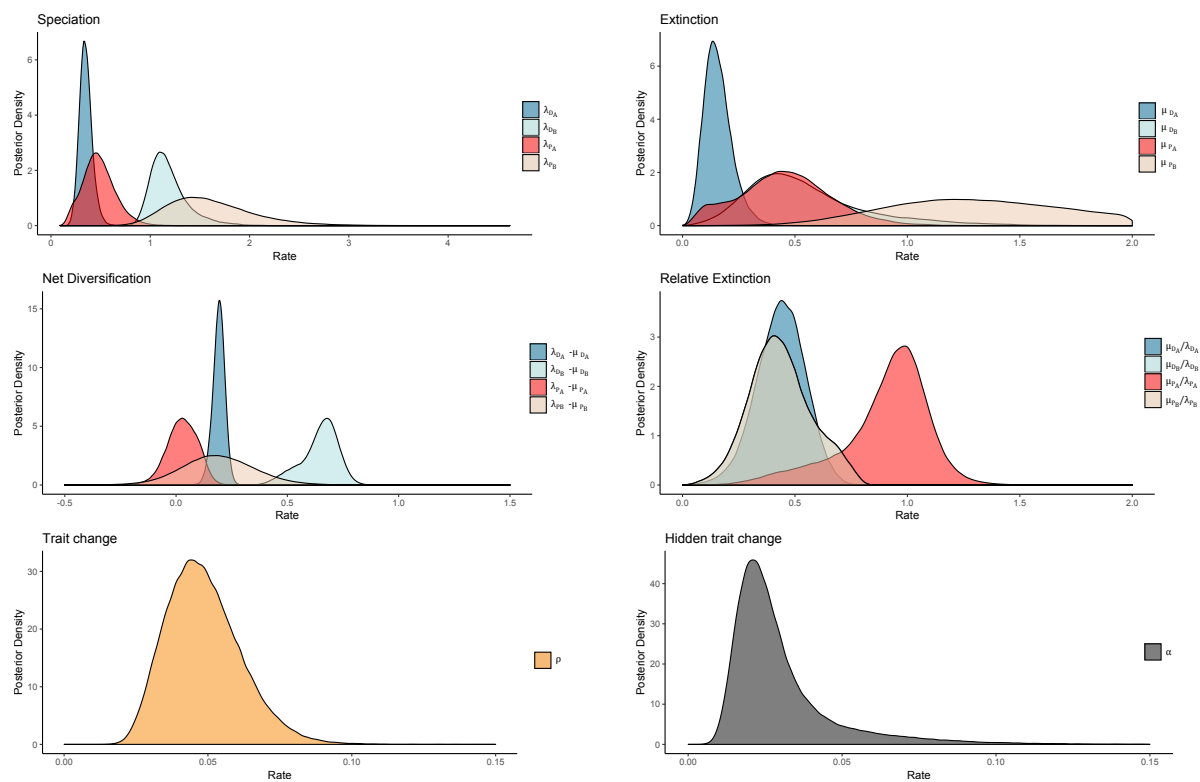
Figure S3: Posterior distribution for each of the parameters in the D/P+A/B, polyploidy model
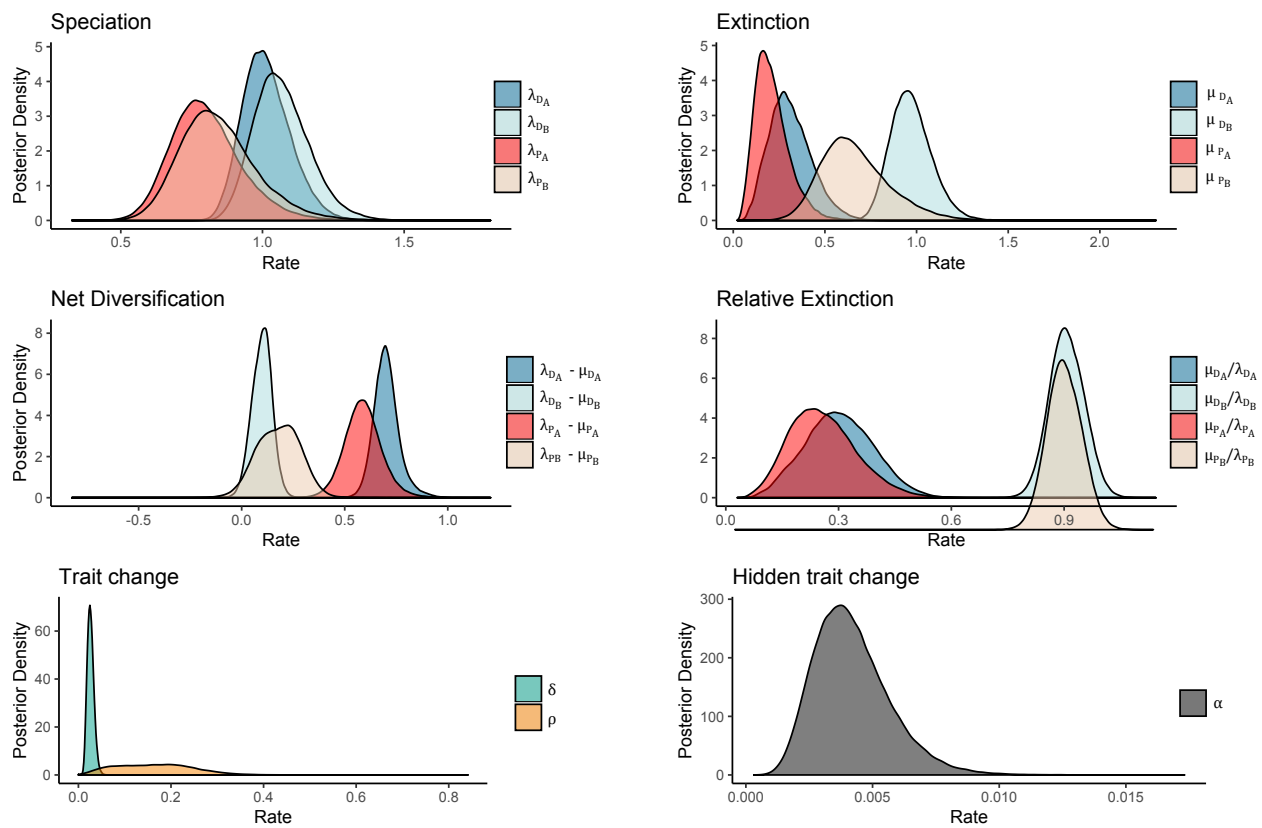
Figure S4: Posterior distribution for each of the parameters in the D/P+$\delta$+A/B, polyploidy model. The axis is offset in one location so that the two overlapping distributions can be seen.
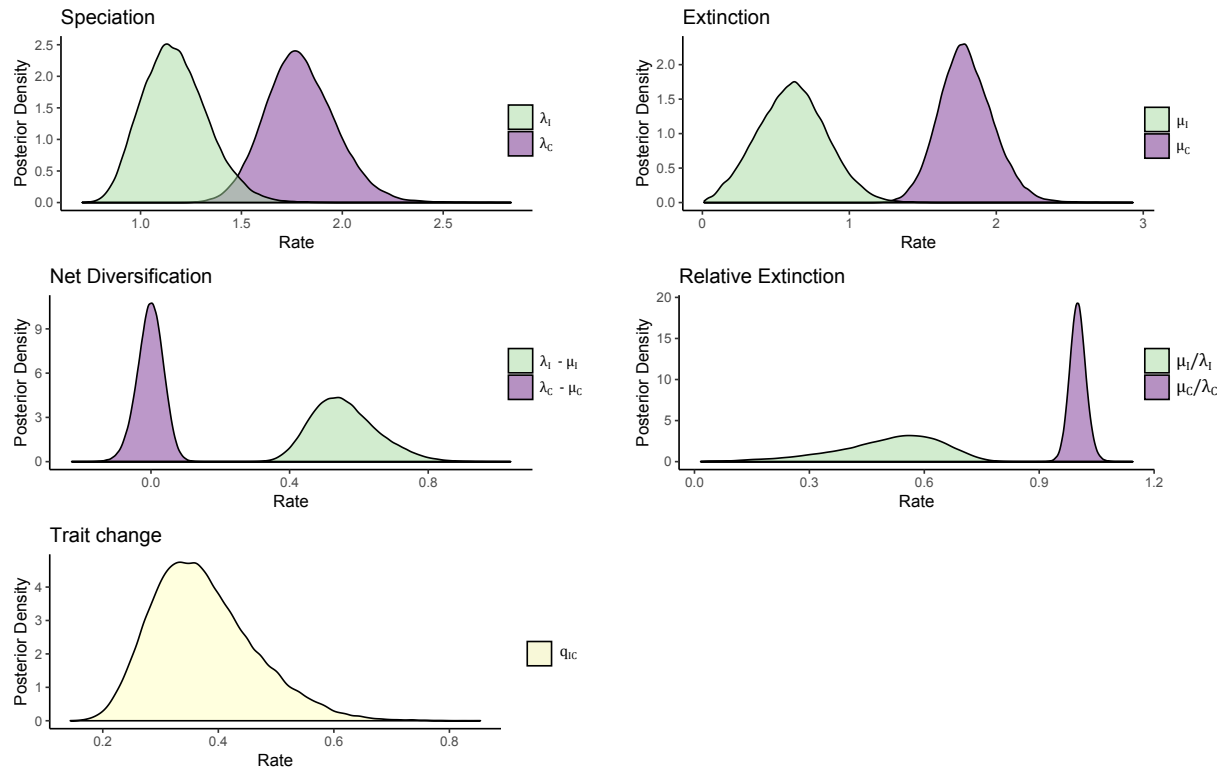
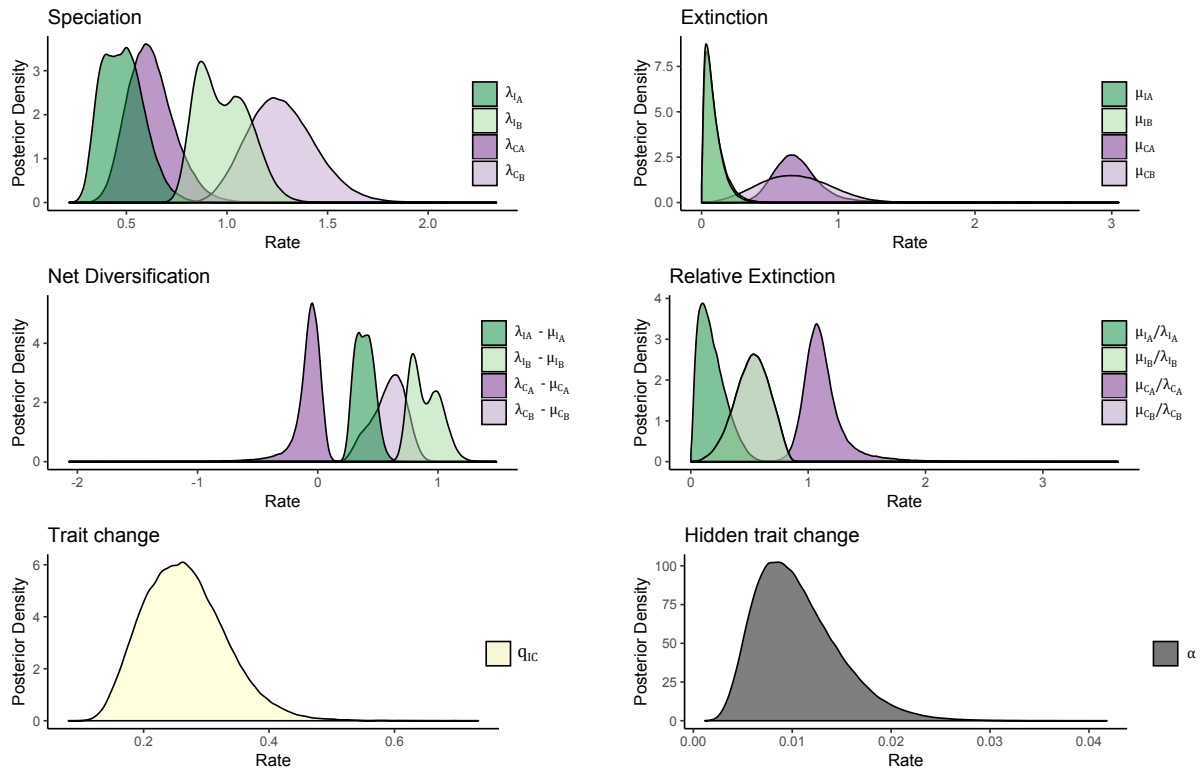Figure S5: Posterior distribution for each of the parameters in the I/C, breeding system model

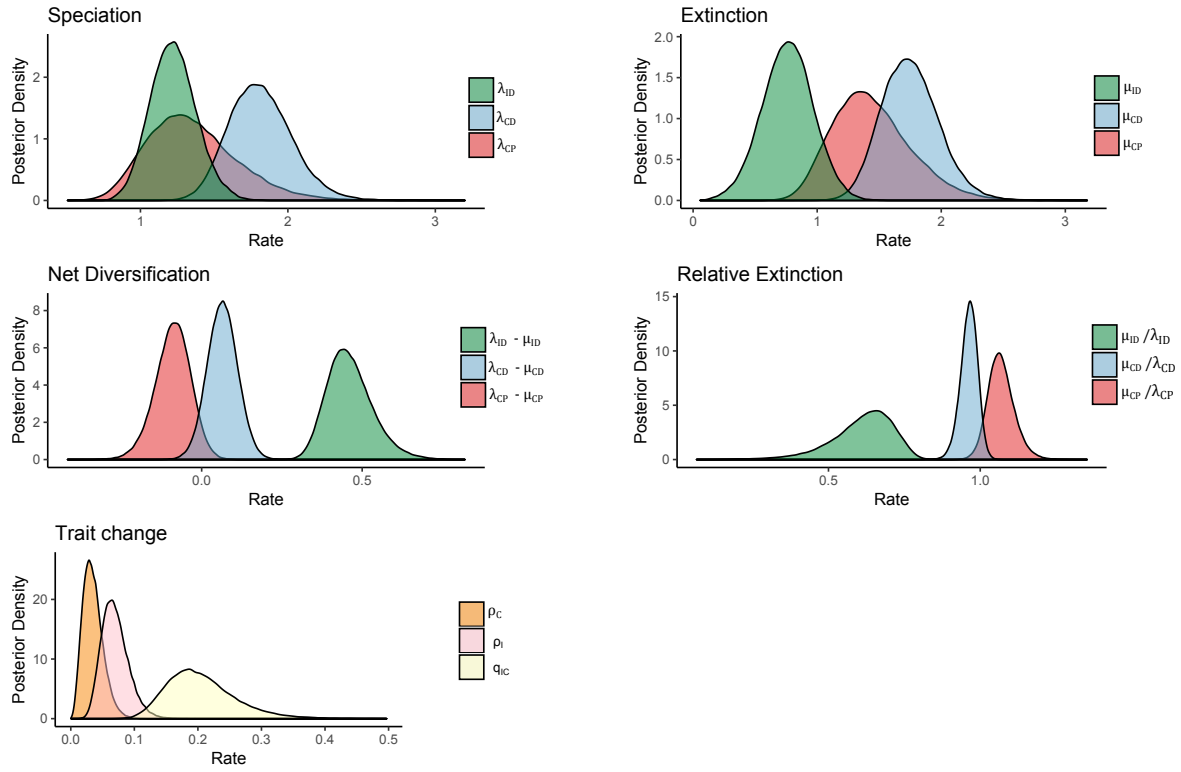Figure S6: Posterior distribution for each of the parameters in the I/C+A/B, breeding system model

Figure S7: Posterior distribution for each of the parameters in the ID/CD/CP, polyploidy and breeding system model
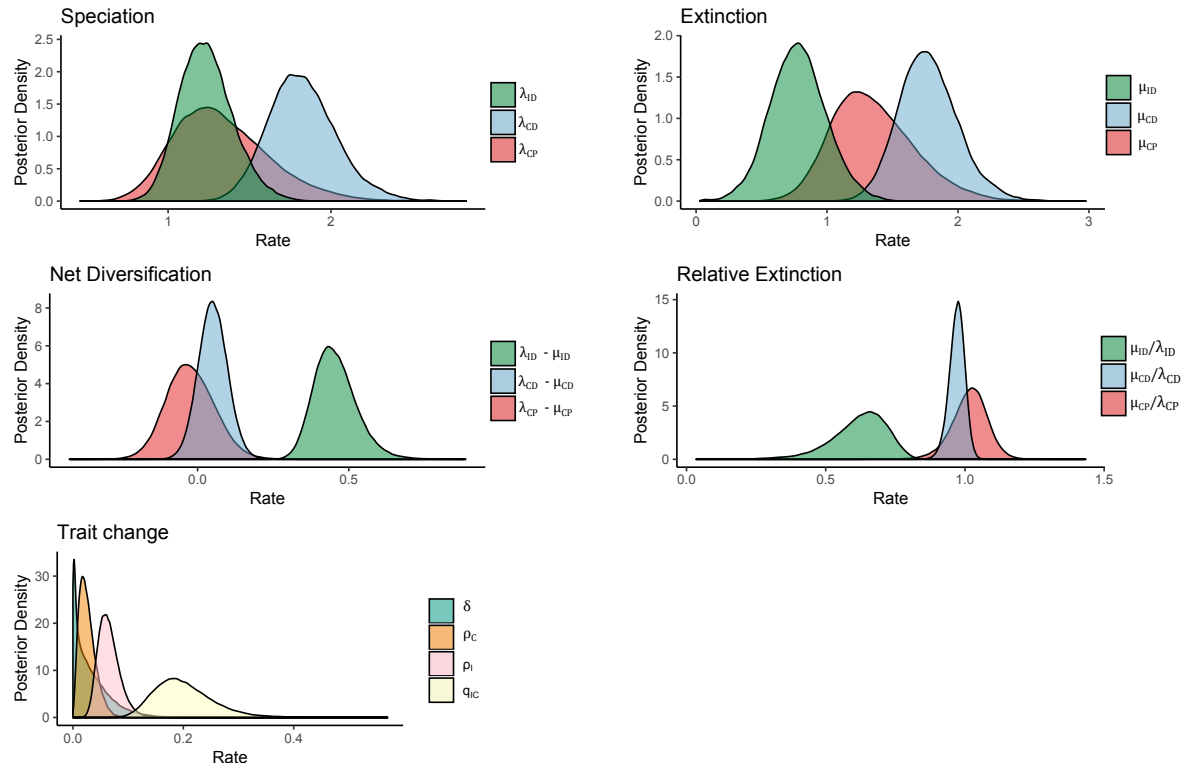
Figure S8: Posterior distribution for each of the parameters in the ID/CD/CP+$\delta$, polyploidy and breeding system model
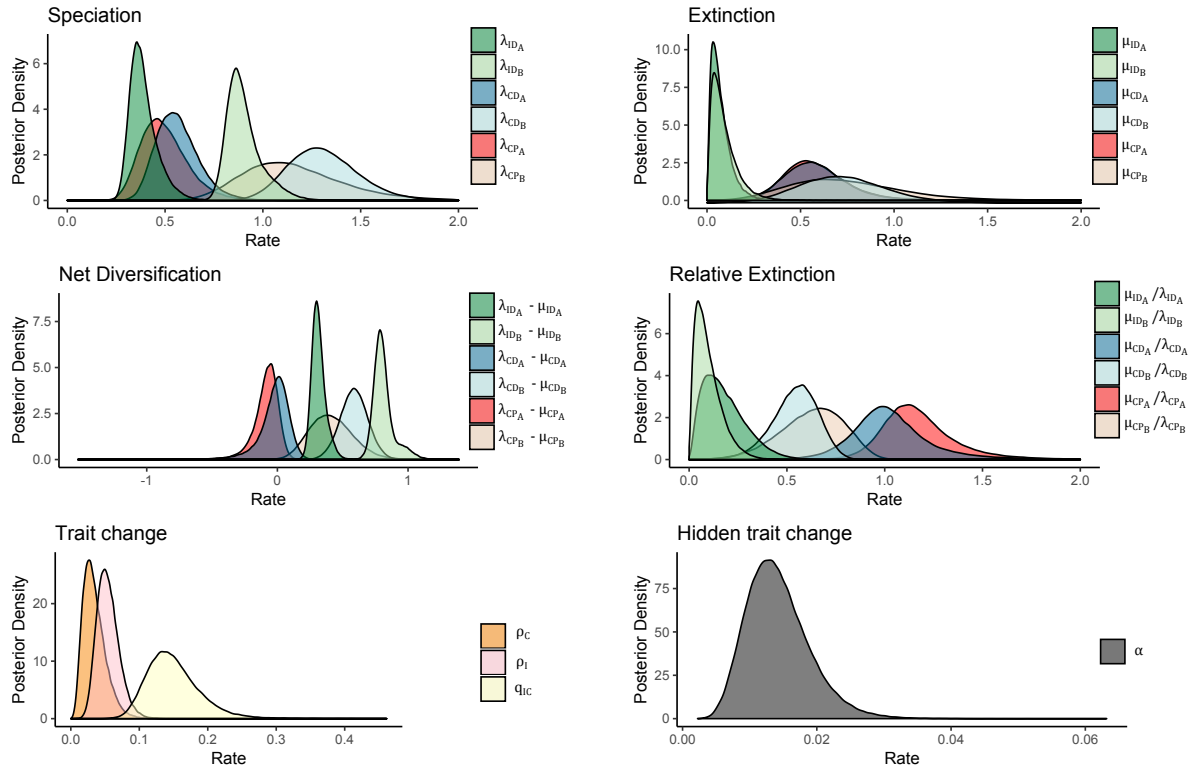
Figure S9: Posterior distribution for each of the parameters in the ID/CD/CP+A/B polyploidy and breeding system model
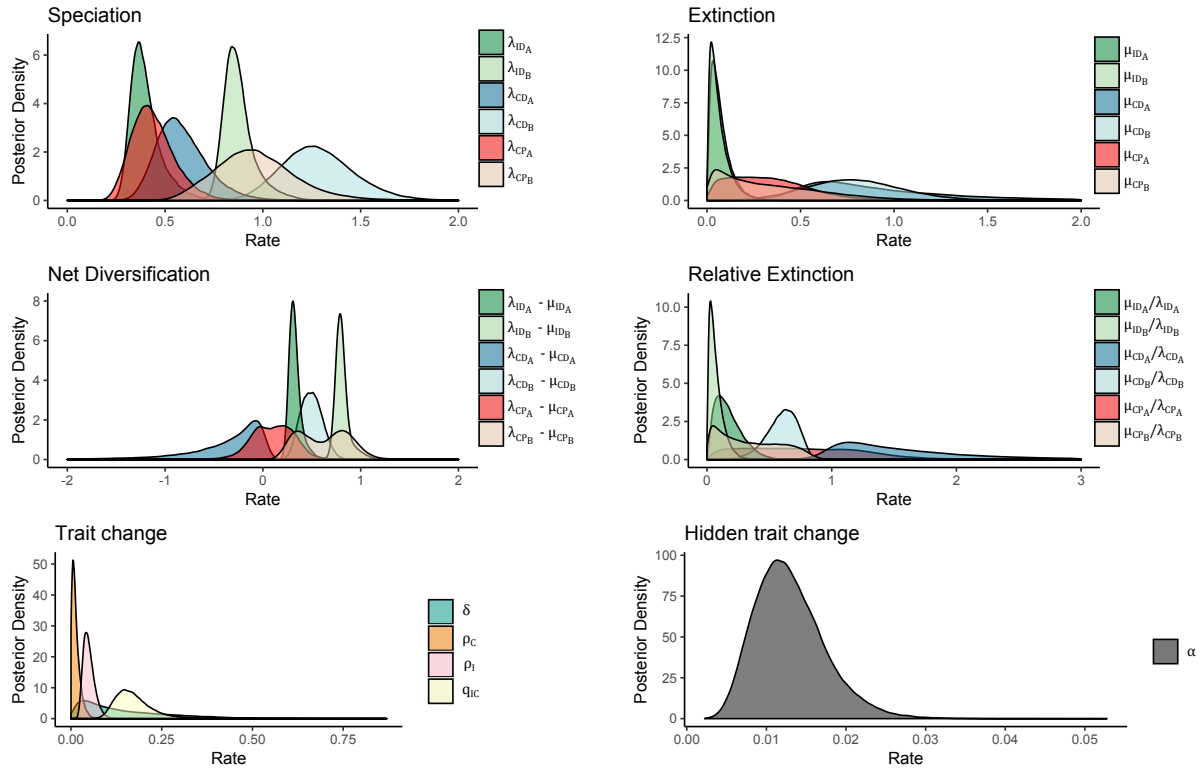
Figure S10: Posterior distribution for each of the parameters in the ID/CD/CP+$\delta$+A/B, polyploidy and breeding system model

| | D/P | D/P+A/B | ID/CD/CP | ID/CD/CP+A/B |
|---|---|---|---|---|
| $r_D$ | 0.260 | 0.193, 0.658 | — | — |
| $r_P$ | -0.056 | 0.030, 0.187 | — | — |
| $r_I$ | — | — | — | — |
| $r_C$ | — | — | — | — |
| $r_{ID}$ | — | — | 0.455 | 0.309, 0.797 |
| $r_{CD}$ | — | — | 0.065 | -0.006, 0.587 |
| $r_{CP}$ | — | — | -0.088 | -0.074, 0.403 |
| $\rho$ | 0.047 | 0.047 | — | — |
| $\rho_I$ | — | — | 0.067 | 0.053 |
| $\rho_C$ | — | — | 0.033 | 0.032 |
| $q_{IC}$ | — | — | 0.198 | 0.145 |

| | D/P | D/P+A/B | I/C | I/C+A/B | ID/CD/CP | ID/CD/CP+A/B |
|---|---|---|---|---|---|---|
| $r_D$ | 0.382 | 0.698, 0.100 | — | — | — | — |
| $r_P$ | 0.109 | 0.587, 0.182 | — | — | — | — |
| $r_I$ | — | — | 0.550 | 0.386, 0.877 | — | — |
| $r_C$ | — | — | -0.001 | -0.059, 0.606 | — | — |
| $r_{ID}$ | — | — | — | — | 0.449 | 0.318, 0.789 |
| $r_{CD}$ | — | — | — | — | 0.050 | -0.248, 0.494 |
| $r_{CP}$ | — | — | — | — | -0.027 | 0.110, 0.634 |
| $\rho$ | 0.033 | 0.026 | — | — | — | — |
| $\rho_I$ | — | — | — | — | 0.063 | 0.047 |
| $\rho_C$ | — | — | — | — | 0.024 | 0.011 |
| $\delta$ | 0.050 | 0.162 | — | — | 0.022 | 0.107 |
| $q_{IC}$ | — | — | 0.364 | | 0.194 | 0.164 |

Table S1: Median rate estimates for all fitted models. Units are per million years. Two comma-separated numbers refer to the *A* and *B* hidden states, and — means the parameter was not present in the model. Net diversification rates ($r$) are subscripted with trait state initials (Diploid, Polyploid, Incompatible, Compatible). Transition rates are $\rho$ (polyploidization), subscripted with background breeding system state; $\delta$ (diploidization); and $q_{IC}$ (loss of self-incompatibility). The upper section is for models without diploidization, and the lower section is for models with diploidization. The supplemental figures show the corresponding distributions of parameter estimates.